

METHODS

Plasmids. Full-length complementary DNAs of human PHF2, ARID5B (full length, β isoform), HNF4 α and FXR were inserted into pcDNA3 vectors (Invitrogen; ref. 11). Deletion mutants of PHF2 (amino acids 1–229 fused to amino acids 367–1103 for PHF2 Δ immC) and ARID5B (amino acids 1–318 fused to amino acids 423–1188 for ARID5B Δ ARID) were amplified by PCR and cloned into pcDNA3 or pGEX4T-1 (Amersham). Point mutants of PHF2 (S1056A point mutation, or S797A, S899A, S954A and S1056A for PHF2 Δ 45A) and PHF2 jmjC-domain point mutants (H249A, Y321A and H338A) and ARID5B were generated by site-directed mutagenesis. HNF4RE-tk-luciferase reporter plasmids were generated by insertion of the promoter region of consensus HNF4RE into a pGL3 luciferase plasmid³². FXRE-tk-luciferase reporter plasmids were generated by insertion of the promoter region of human SHP (–572 to –3) containing FXRE into a pGL3 luciferase plasmid. Other plasmids have been described previously^{11,12,32,33}.

Biochemical purification and separation of FXR- or PHF2-associated complexes. The hepatic tumour-derived HepG2 cells were incubated for 4 h with either FSK (1 μ M) and/or H89 (1 μ M), and the nuclear extracts were prepared as previously described. For purification of the FXR-associating complex, the nuclear extracts were bound to glutathione S-transferase (GST)–FXR(D/E)–His (amino acids 193–477) columns^{11,12,33}. The bound complexes were eluted with reduced glutathione (15 mM) in elution buffer. Glycerol density gradients were carried out as previously described^{11,12,33}. The complex fraction was further loaded onto a diethylaminoethyl column (Whatman), and eluted with different concentrations of NaCl (150 mM–1 M). The purified proteins were silver-stained, and identified by matrix-assisted laser desorption/ionization–time of flight mass spectrometry (Bruker)^{11,12,33}. For purification of PHF2-associating complex, the nuclear extracts were loaded onto M2 anti-Flag agarose gel (Sigma, A2220, 069K6018). After washing with binding buffer, the bound proteins were eluted by incubation with 1.0 ml of the Flag peptide ((EYKEEKK)₂, 0.2 mg ml^{–1}) (Sigma).

In vitro and in vivo lysine demethylation assay. The *in vitro* histone demethylation assays were carried out as previously described^{7,10}.

For preparation of demethylases from mammalian cells, 293F cells were transfected with Flag–PHF2 plasmid using Lipofectamine 2000 (Invitrogen). After 36 h, the cells were lysed with TNE (20 mM Tris at pH 7.8, 150 mM NaCl, 0.5 mM EDTA, 1% NP40). For phosphorylation of PHF2 *in vivo*, cells were treated with FSK (10^{–6} M) 2 h before harvest, and NaF/Na₂VO₃ added to TNE. Cell lysates were subjected to immunoprecipitation using anti-Flag antibody-conjugated beads (Sigma, A2220, 069K6018). Beads were washed three times with high-salt TNE (20 mM Tris at pH 7.8, 450 mM NaCl, 0.5 mM EDTA, 1% NP40), and then three times with EDTA-free TNE. For phosphorylation of PHF2 *in vitro*, beads were mixed with 20 μ l PKA buffer (0.1 μ g PKA (Upstate), 20 mM Tris at pH 7.5, 10 mM MgCl₂, 100 μ M ATP and incubated for 1 h at 37 °C. Then, beads were washed three times with demethylase stock buffer (20 mM Tris at pH 7.5, 150 mM KCl, 10% glycerol). The prepared PHF2 protein was used immediately for the demethylation reaction. Alternatively, the purified proteins were eluted with Flag elution buffer (200 mg ml^{–1} Flag peptide, 20 mM Tris at pH 7.5, 450 mM KCl, 10% glycerol).

For preparation of recombinant proteins, recombinant Flag–PHF2 was purified using Bac-to-Bac baculovirus expression systems (Invitrogen) according to the manufacturer's instructions. The purified Flag–PHF2 complex was prepared as described in the section on biochemical purification.

For demethylase reaction, 2 μ g of PHF2 protein or 0.2 μ g of PHF2 complex was mixed with substrates (calf thymus histone (10 μ g) (Sigma, H9250), purified mononucleosome (10 μ g), Flag–ARID5B protein purified from 293F cells (2 μ g) or dimethyl H3 (Lys 9) peptide 1–21 (0.2 μ g) (Upstate 12–430)) in the reaction buffer (final volume 20 μ l) (20 mM Tris-HCl at pH 7.5, 150 mM KCl, 50 μ M Fe(NH₄)₂(SO₄)₂–6H₂O, 1 mM α -ketoglutarate, 1 mM ascorbate, 20 μ M ZnCl₂). The mixtures were incubated at 37 °C for 12 h, terminated by boiling for 5 min in SDS sample buffer^{7,10}. The histone modification or methylation of ARID5B was detected by specific antibodies (see the antibody section). The signal intensity of western blots was quantified using Scion Image.

For histone demethylase assay detecting formaldehyde release, purified PHF2 complex (0.2 μ g) was incubated with native histones (10 μ g) for 30 min according to the manufacturer's protocol using DetectXTM (LUMINOS, K010-F1).

For *in vivo* histone demethylation assay, cells were first lysed in TNE, and the pellet fraction was resuspended in TNE and sonicated for 20 s (Tomy SEIKO) to obtain the chromatin fraction^{3,9,10,34}.

Antibodies, immunoprecipitation and western blotting. Anti-PHF2 and anti-ARID5B polyclonal antibodies were raised against PHF2 peptides (5'-ERSVDVTDVTKQKDC-3', 5'-CKPKPVRDEYEVSD-3', 5'-CAYKSDSSDE-GSLH-3') and ARID5B peptides (5'-CDTPQGRNSDHGEDE-3', 5'-CTDQGSNSEK-

VAEEA-3', 5'-CEQTSKYPSRDMYRE-3'), respectively, by Operon Biotechnology. Anti-ARID5B K336Me2 antibody was raised using the dimethylated peptide (MKER(KMe2)TPIER: ARID5B K336Me2), and purified over a peptide affinity column (MBL). The antibodies that bound to the non-methylated peptide (MKERKTPIER) were removed using an affinity column. The specificity of the antibody toward K336Me2 over K336Me0, Me1 and Me3 peptides was determined in Supplementary Fig. S20 using enzyme-linked immunosorbent assays (MBL).

For immunoprecipitation, cells were treated with FSK (1 μ M) or glucagon (200 nM) for 2 h and cells were lysed in TNE. Cell lysates were incubated with the indicated antibodies listed in Supplementary Table S1. A full list of antibodies and the dilutions used is given in Supplementary Table S1.

Cell culture, transfection and luciferase assays. Mouse immortalized hepatocytes, TLR2 cells, were obtained from RIKEN (cell no. RCB0750; ref. 35). The immortalized hepatocytes were cultured at 33 °C in DMEM containing 2% fetal bovine serum, 10 μ g ml^{–1} transferrin, 1 μ g ml^{–1} insulin and 10 ng ml^{–1} epidermal growth factor, using collagen-coated dishes. Other cell lines are cultured in DMEM supplemented with 10% fetal bovine serum. Cells were treated with glucagon (200 nM), FSK (1 μ M), H89 (1 μ M), CHX (1 μ M), GW4064 (1 μ M), dexametazone (10 nM) or 25-OH cholesterol (10 μ g ml^{–1}) either for 24 h (luciferase assays), for 6 h (*in vivo* demethylation assays) or for 2 h (immunoprecipitation).

For luciferase assays, cells at 40–50% confluence were transfected with the indicated plasmids (0.25 μ g reporter plasmids, 0.1 μ g HNF4 α , 0.1 μ g FXR, 0.05 μ g of PHF2) using Lipofectamine reagent (Gibco BRL). Luciferase activity was determined with the luciferase assay system (Promega) as previously described^{11,12,32,33}.

ChIP experiments. ChIP assays were carried out essentially as previously described^{11,12,33}. Hepatocytes were treated with glucagon (200 nM), FSK (1 μ M) and/or H89 (1 μ M) for 4 h or as indicated. Then, cells were subjected to ChIP experiment as described¹¹. The precipitated DNA fragments were amplified by quantitative PCR (qPCR; TAKARA). For qPCR with reverse transcription, the specific primer sets were designed and provided by TAKARA. The primer sets are shown in Supplementary Table S1.

Fasting responses in mice. All mice were maintained according to the protocol approved by the Animal Care and Use Committee of the University of Tokyo.

For ChIP assays¹¹, eight-week-old C57BL/6 male mice were either deprived of food or fed for 6 h. Livers were isolated, minced and fixed in PBS containing 1% formaldehyde at 4 °C overnight. The cells were washed in PBS twice, then sonicated in PBS containing 0.2 mM EDTA and 1% Triton X-100. The cell lysates were subjected to ChIP assays as previously described¹¹.

RNA isolation and qPCR. Messenger RNA was isolated as previously reported³³. For qPCR with reverse transcription, the specific primer sets were designed and provided by TAKARA. The primer sequences are shown in Supplementary Table S1, and the amount was normalized using glyceraldehyde-3-phosphate dehydrogenase.

RNA interference experiments. The siRNAs as shown in Supplementary Table S1, together with siCONTROL non-targeting siRNA no. 2 (catalogue no. D-001210-02-20), were synthesized by and obtained from Dharmacon/Thermo, and were transfected using Lipofectamine 2000 reagent (Invitrogen) as previously described¹¹. The two siRNAs used for each experiment, and the results of target sequence no. 1 (for PHF2, ARID5B and HNF4 α) are shown.

Immunostaining. Immunostaining was carried out essentially as previously described³⁶. 293F cells were transfected with PHF2 or its derivatives, and 12 h after the transfection the cells were treated with FSK for 6 h, then fixed and subjected to immunostaining³⁶. Antibodies used are described in the antibody section.

In vitro and in vivo kinase assays. Recombinant GST–PHF2 deletion mutants expressed in *Escherichia coli* (1 μ g), or Flag–PHF2 and its derivatives (1 μ g) immunoprecipitated from 293F cells using anti-Flag antibody and eluted by Flag peptide, were incubated with PKA (Upstate; 2 ng) in reaction buffer (20 mM Tris-HCl at pH 7.5, 10 mM MgCl₂, γ -³²P ATP) in the presence or absence of PKA inhibitor (10 μ M H89) for 15 min at 30 °C.

For detection of phosphorylated proteins in cells, hepatocytes were treated with the indicated ligands for 2 h, then subjected to phospho-protein purification using a PhosphoProtein Purification Kit (QIAGEN; ref. 12). Alternatively, cell lysates were immunoprecipitated using anti-PHF2 or anti-Flag as indicated, then western

blotted using anti-phospho-PKA-substrate antibody (Cell Signaling Technology, 100G7E, 9624S). For statistical analysis, the signal intensity of western blots was quantified using Scion Image, and the average \pm s.d. of four independent experiments was shown with Student's *t*-test.

DNA precipitation assays. DNA precipitation assays were carried out essentially as described^{33,37}. Human *Pck1* promoter (−312 ~ 23) was amplified by PCR using biotinylated primers. Then, the biotinylated DNA was annealed and bound to avidin beads (Invitrogen). 293F cells were transfected with Flag-ARID5B, HA-PHF2 and their derivatives, and incubated with/without FSK for 2 h. Cell lysates were incubated with the DNA-bound avidin beads for 30 min in TNE buffer. The samples were subjected to western blotting^{33,37}.

32. Unno, A. *et al.* TRRAP as a hepatic coactivator of LXR and FXR function. *Biochem. Biophys. Res. Commun.* **327**, 933–938 (2005).
33. Ohtake, F. *et al.* Modulation of oestrogen receptor signalling by association with the activated dioxin receptor. *Nature* **423**, 545–550 (2003).
34. Yokoyama, A., Takezawa, S., Schule, R., Kitagawa, H. & Kato, S. Transrepressive function of TLX requires the histone demethylase LSD1. *Mol. Cell Biol.* **28**, 3995–4003 (2008).
35. Puigserver, P. *et al.* Insulin-regulated hepatic gluconeogenesis through FOXO1-PGC-1 α interaction. *Nature* **423**, 550–555 (2003).
36. Okada, M. *et al.* Switching of chromatin-remodelling complexes for oestrogen receptor-alpha. *EMBO Rep.* **9**, 563–568 (2008).
37. Fujiki, R. *et al.* Ligand-induced transrepression by VDR through association of WSTF with acetylated histones. *EMBO J.* **24**, 3881–3894 (2005).

DOI: 10.1038/ncb2228

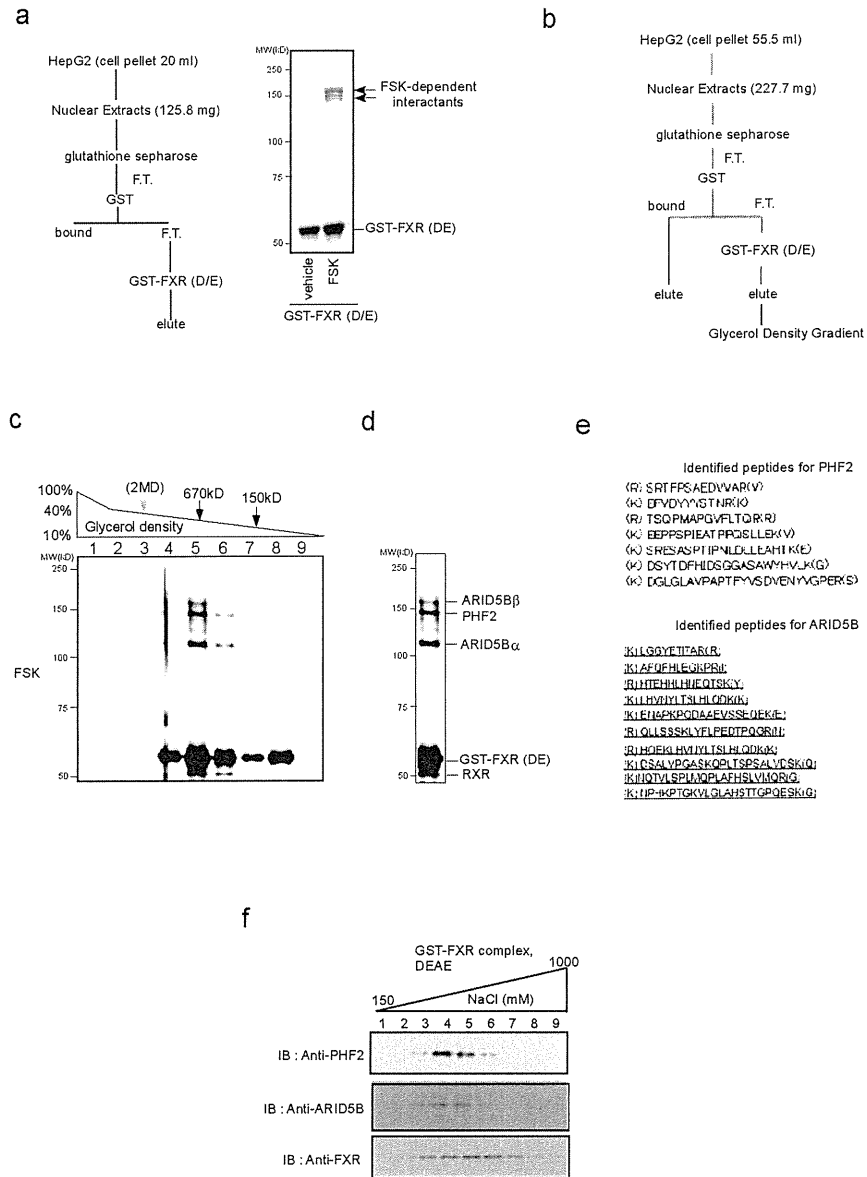


Figure S1 Purification of PHF2/ARID5B complex. **a**, Purification of a signal-dependent GST-FXR-associated proteins from HepG2 cells. Nuclear extracts from FSK-treated HepG2 cells were loaded on GST-FXR-bound glutathione sepharose beads. The bound proteins were analyzed by silver staining. **b**, The scheme for the purification of nuclear receptor-associated complexes. The experimental details were supplied in the supplemental methods. **c**, Purification of a GST-FXR-associated complex from HepG2 cells. Nuclear

extracts from FSK-treated HepG2 cells were loaded on GST-FXR-bound glutathione sepharose beads. The eluted complexes were separated by glycerol density gradients as indicated. **d**, **e**, The isolated complexes were silver stained, and each protein was identified by MALDI-TOF/MS and fingerprinting. **f**, PHF2 and ARID5B form a complex with GST-FXR. The purified GST-FXR-associated complex in (c) was further separated by DEAE column with different NaCl concentrations. The elutants were subjected to Western blotting.

SUPPLEMENTARY INFORMATION

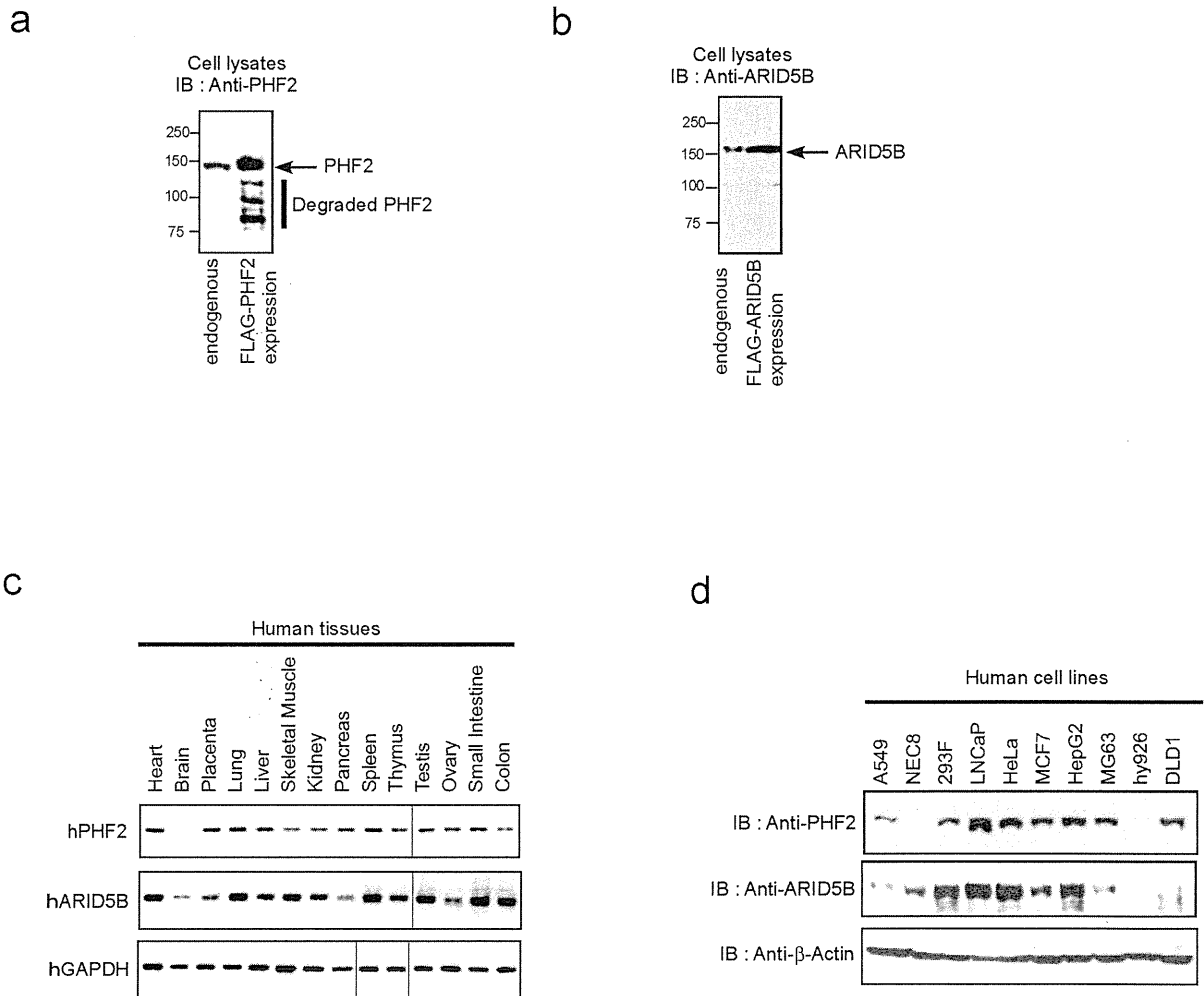


Figure S2 The expression profiles of PHF2 and ARID5B. **a, b**, Specificity confirmation of the newly raised antibodies. Normal 293F cell lysates or lysates transfected with the indicated expression vectors were subjected to Western blotting. This confirmed that these anti-PHF2 (**a**) and anti-ARID5B (**b**) antibodies detect endogenous proteins with high specificity. **c**, The mRNA expression profiles of human PHF2 and ARID5B. The mRNA levels

of PHF2 and ARID5B were determined by semi-quantitative PCR using cDNAs from human tissues (Clontech, human cDNA panel, #636742 and #636743). **d**, Protein expression of PHF2 and ARID5B in various human cell lines. Total cell lysates were prepared from the indicated human cell lines. Equal amounts of proteins were subjected to Western blotting with the indicated antibodies.

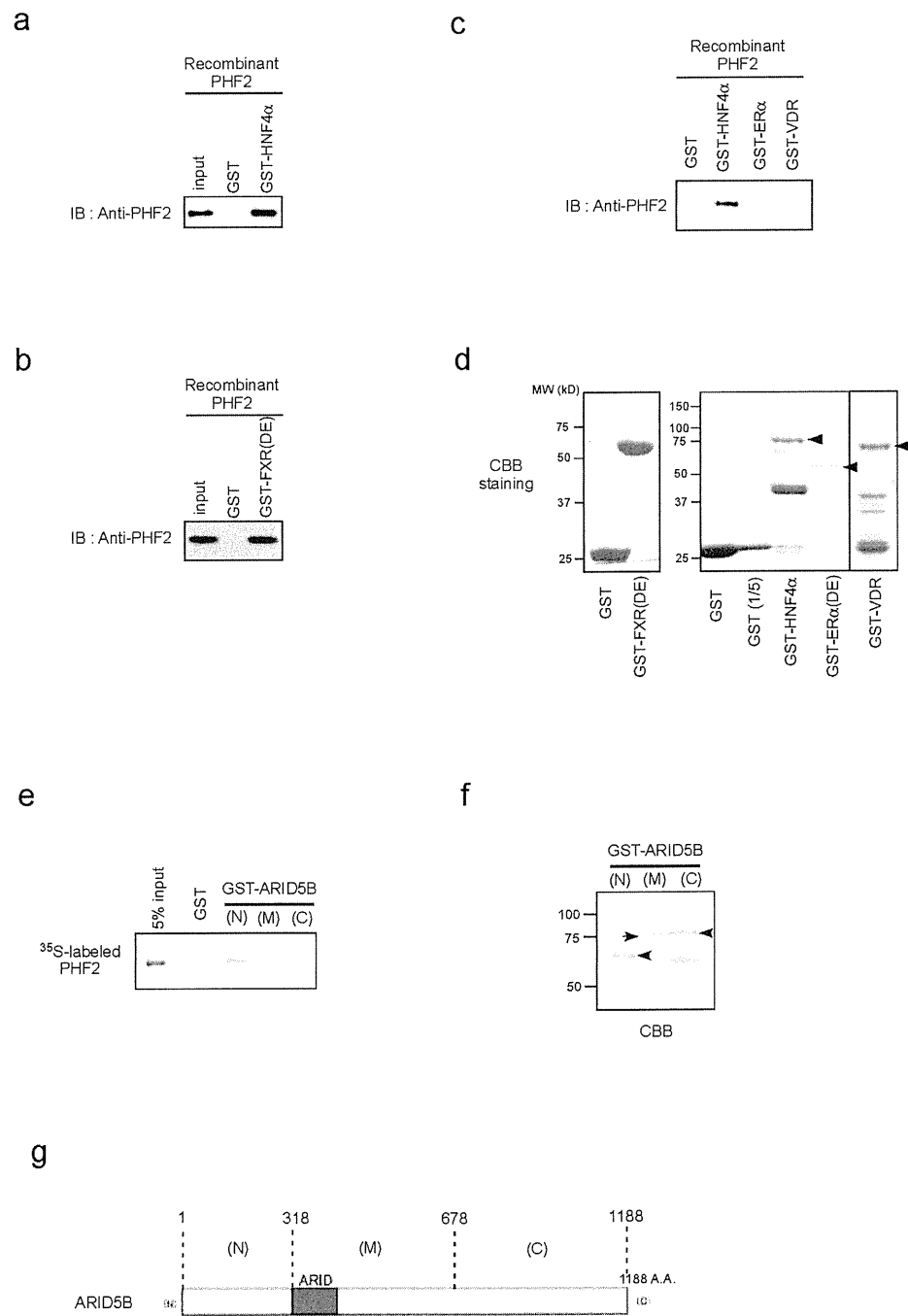


Figure S3 Direct association of PHF2/ARID5B with HNF4 α and FXR. **a-d**, GST pull-down assay with recombinant PHF2 protein and GST-tagged FXR(DE), HNF4 α , ER α (DEF), or VDR. Bound protein was detected with anti-PHF2 antibody. **e-g**, GST pull-down assay with 35 S-labeled PHF2 and GST-ARID5B mutants. GST-ARID5B mutants, described in (g), were incubated with *in vitro*-translated PHF2. Bound proteins were detected by autoradiography.

SUPPLEMENTARY INFORMATION

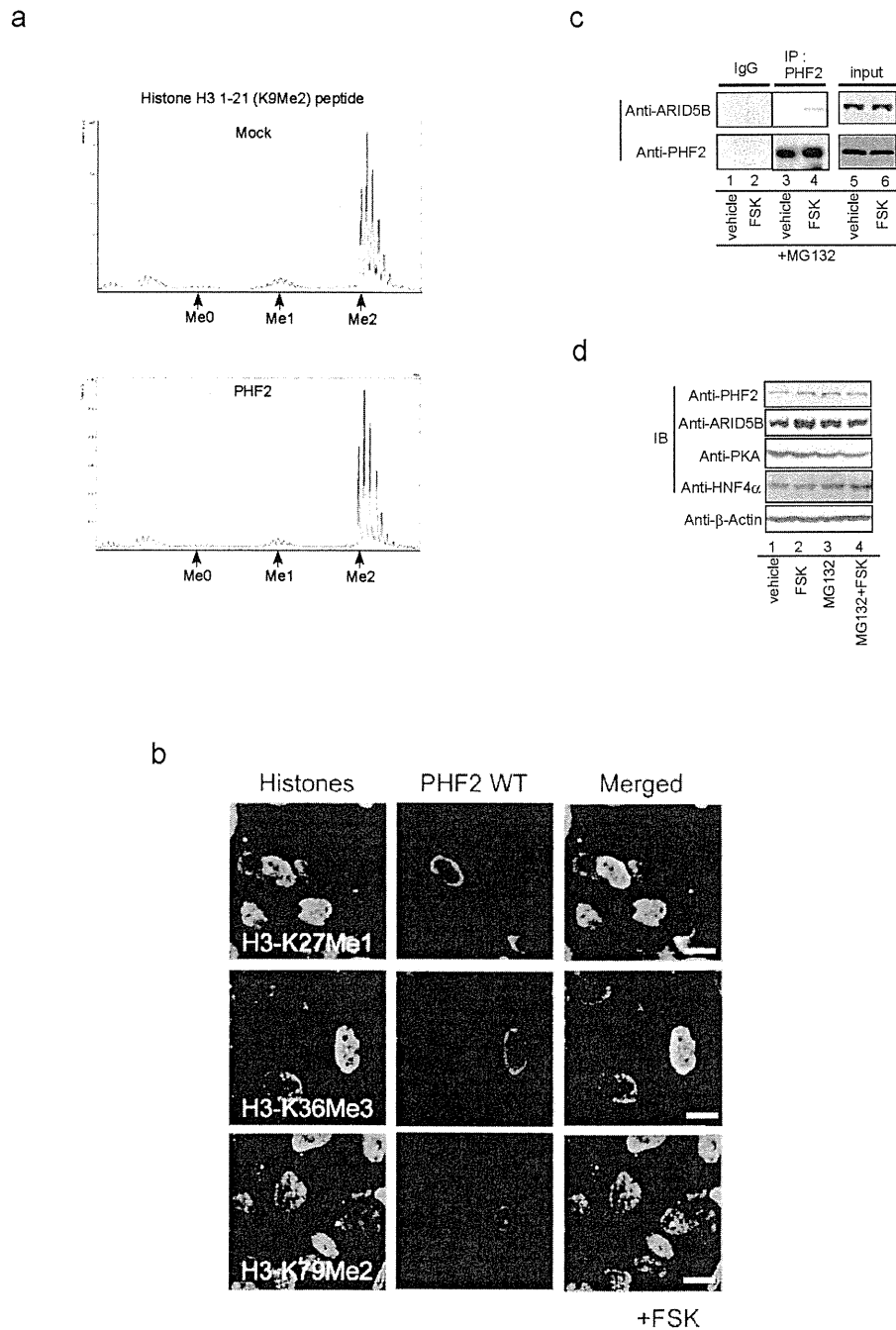


Figure S4 Demethylation activity of PHF2. **a**, Demethylase assay with H3 peptide. Purified PHF2 protein or mock immunoprecipitants incubated with PKA as in Fig. 3b was subjected to the demethylase assay with 0.2 μ g of biotin-conjugated dimethyl histone H3 (Lys9) peptide (residues 1-21) (Upstate, 12-430). Demethylation was determined using MALDI-TOF/MS. Detailed methods were supplied as supplementary methods. **b**,

Immunostaining of 293F cells was performed as described in Fig. 1f. **c**, Hepatocytes were treated with FSK (10^{-6} M) and MG132 (10^{-5} M) for two hrs. Total cell lysates were subjected to immunoprecipitation as indicated. **d**, FSK treatment did not alter protein expression levels of PHF2, ARID5B, or HNF-4 α . Hepatocytes were treated with FSK (10^{-6} M) or MG132 (10^{-5} M) as indicated for 6 hrs. Cell lysates were subjected to Western blotting.

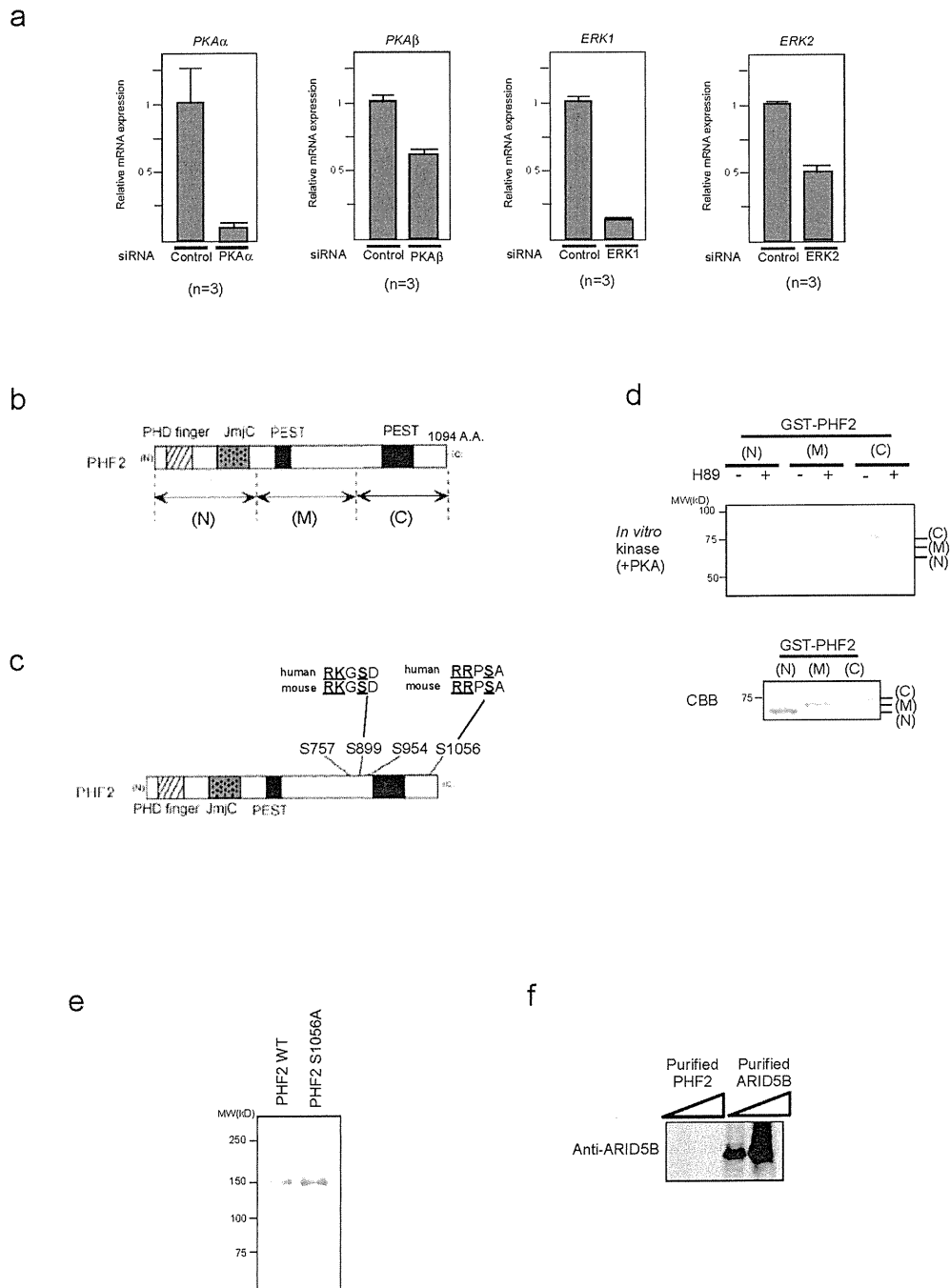


Figure S5 PKA phosphorylates PHF2 *in vitro* and *in vivo*. **a**, As controls for Fig. 2d, expression levels of the indicated genes were quantified by qPCR. Data shows average \pm S.D. (n=3). **b**, The schematic representation of deletion mutants of PHF2 used. **c**, The schematic representation of phosphorylation sites within PHF2 determined in Figure 2. **d**, PHF2 is phosphorylated by PKA at C-terminal region *in*

in vitro. *In vitro* kinase assay as indicated. **e**, 293F cells were transfected with FLAG-PHF2 or its mutant, and PHF2 was purified to of near homogeneity using anti-FLAG affinity column. Purified proteins were subjected to silver staining as indicated. **f**, Purified protein in Fig. 3a were subjected to Western blotting. Note that purified PHF2 did not include ARID5B.

SUPPLEMENTARY INFORMATION

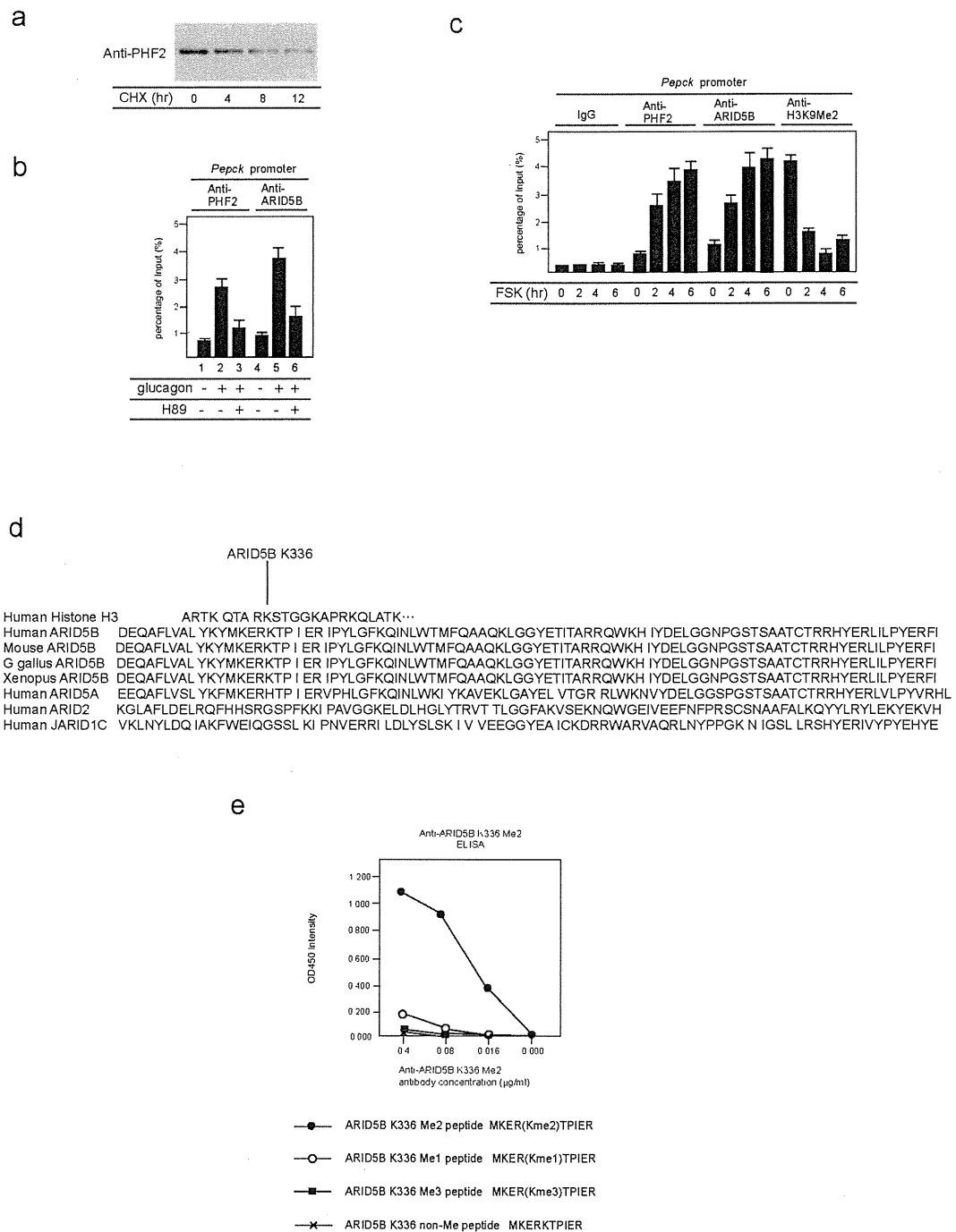


Figure S6 Promoter recruitment of PHF2/ARID5B. **a**, Protein turn-over of PHF2 as revealed by cycloheximide treatment. **b**, Recruitment of PHF2 and ARID5B to the *Pepck* promoter was abolished by a PKA inhibitor, H89. Hepatocytes were treated with glucagon and/or H89 (1 µM) for four hrs, then ChIP assay was performed using the indicated antibodies. **c**, Co-recruitment of PHF2/ARID5B and demethylation of H3K9Me2 in *Pepck* promoter over similar time courses. Hepatocytes were treated with FSK for the indicated time, then a ChIP assay was performed as indicated. **d**, The schematic

representation of amino acid sequences of ARID5B and other ARID family proteins. The sequence of histone H3K9 is also represented. **e**, Specificity of anti-ARID5B K336Me2 antibody. A rabbit polyclonal antibody against di-methylated Lys336 of ARID5B (anti-ARID5B K336Me2) was raised by using the di-methylated peptide [ARID5B K336Me2; MKER(Kme2)TPIER], and purified over a peptide-affinity column. The specificity of antibody toward K336Me2 peptide over non-methylated, mono-methylated, or tri-methylated peptides was determined by ELISA assays.

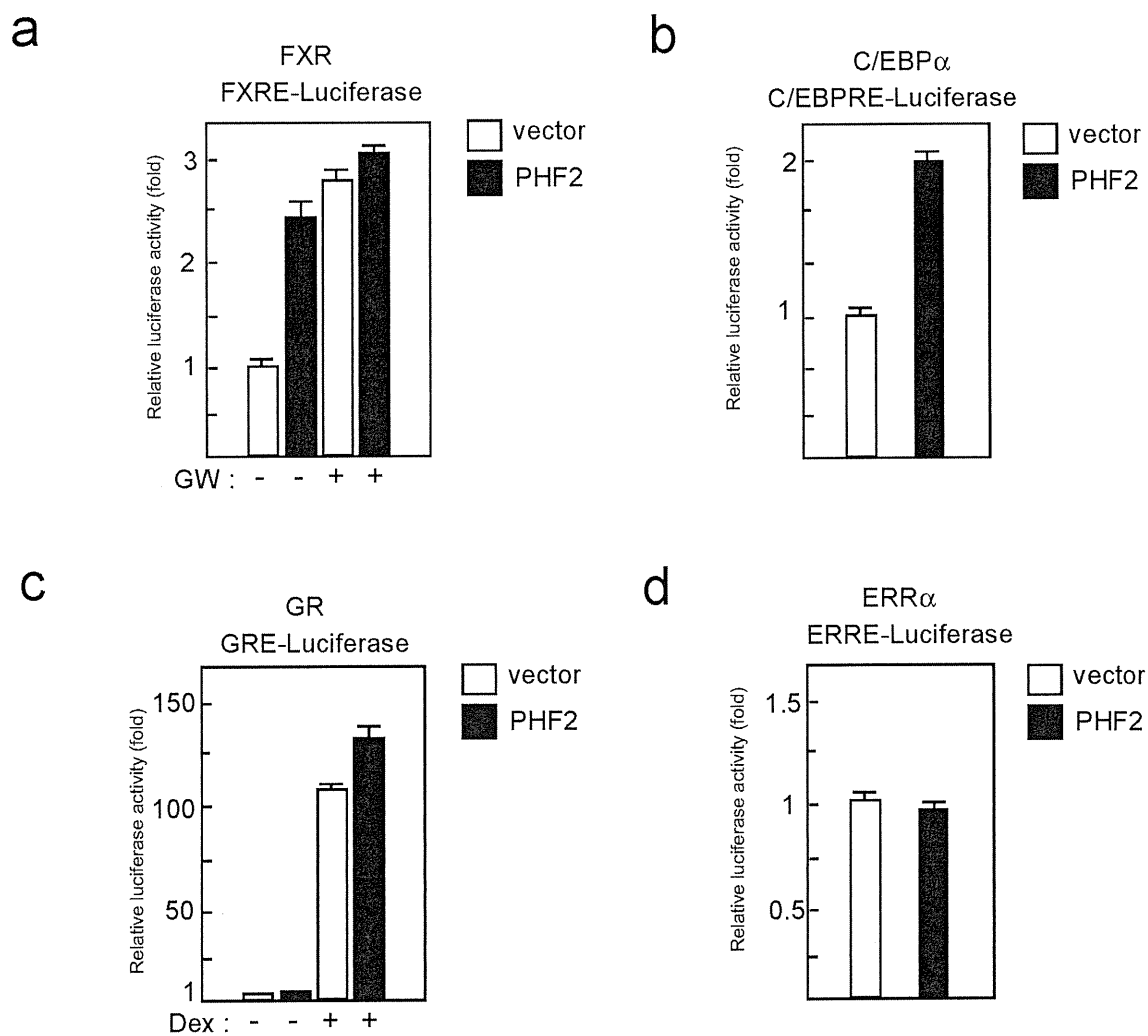


Figure S7 Co-activator activity of PHF2 for known gluconeogenic-related transcription factors. 293F cells were transfected with the indicated expression vectors and reporter plasmids with or without PHF2. Cells were treated with FSK for 24 hrs, then Luciferase assay were performed as indicated.

SUPPLEMENTARY INFORMATION

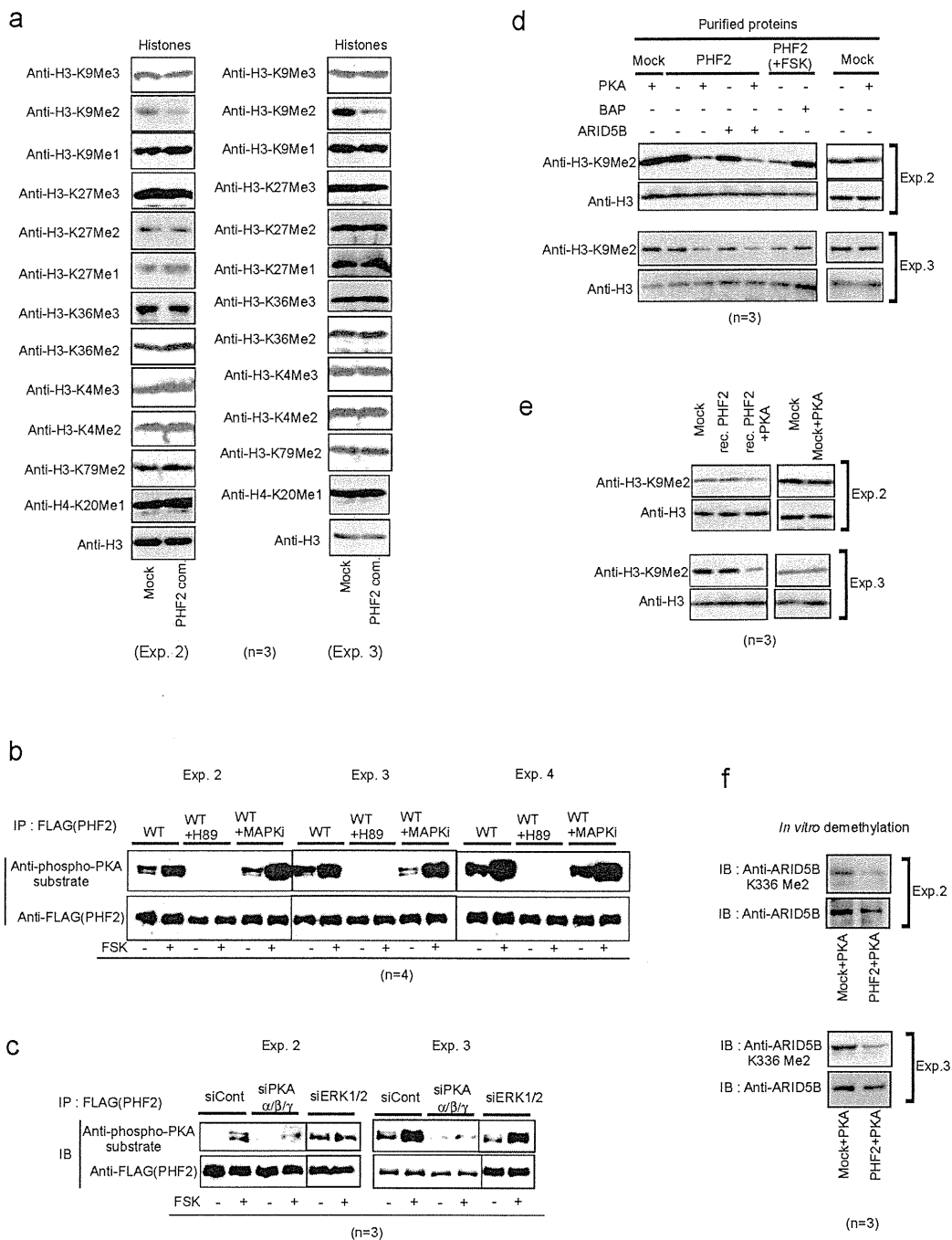


Figure S8 Western blot data for quantification. **a**, For *in vitro* demethylation assay and quantification in Fig. 1c-d, three independent experiments were performed, and histone methylation marks were analyzed by Western blotting as shown in Fig. 1d. The other two sets of data for quantification are shown. **b-c**, Quantification analysis for PKA-mediated phosphorylation of PHF2. Assay was performed as in Fig. 2d, and the other data for quantification in Fig. 2d (left, n=4 and right,

n=3) were shown. **d-e**, Quantification analysis for PKA-dependent PHF2 demethylase activity. Three independent assays were performed as in Fig. 3b-c and 3e-f, and the other two sets of data for quantification (n=3) were shown. **f**, Quantification analysis for demethylation of ARID5B by PHF2 *in vitro*. Three independent assays were performed as in Fig. 5e, and the other two sets of data for quantification in the lower panel of Fig. 5e (n=3) were shown.

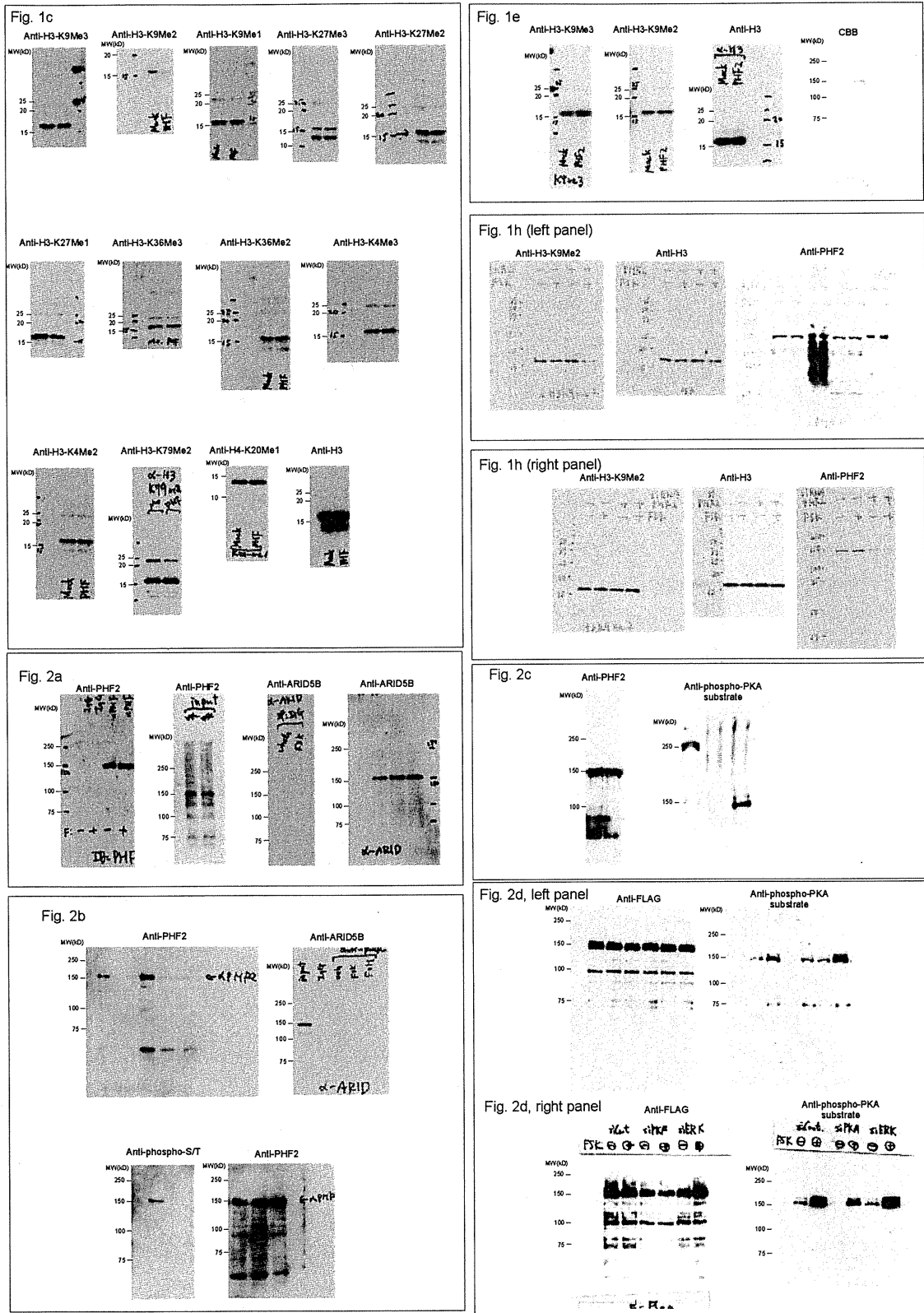


Figure S9 Full scans

SUPPLEMENTARY INFORMATION

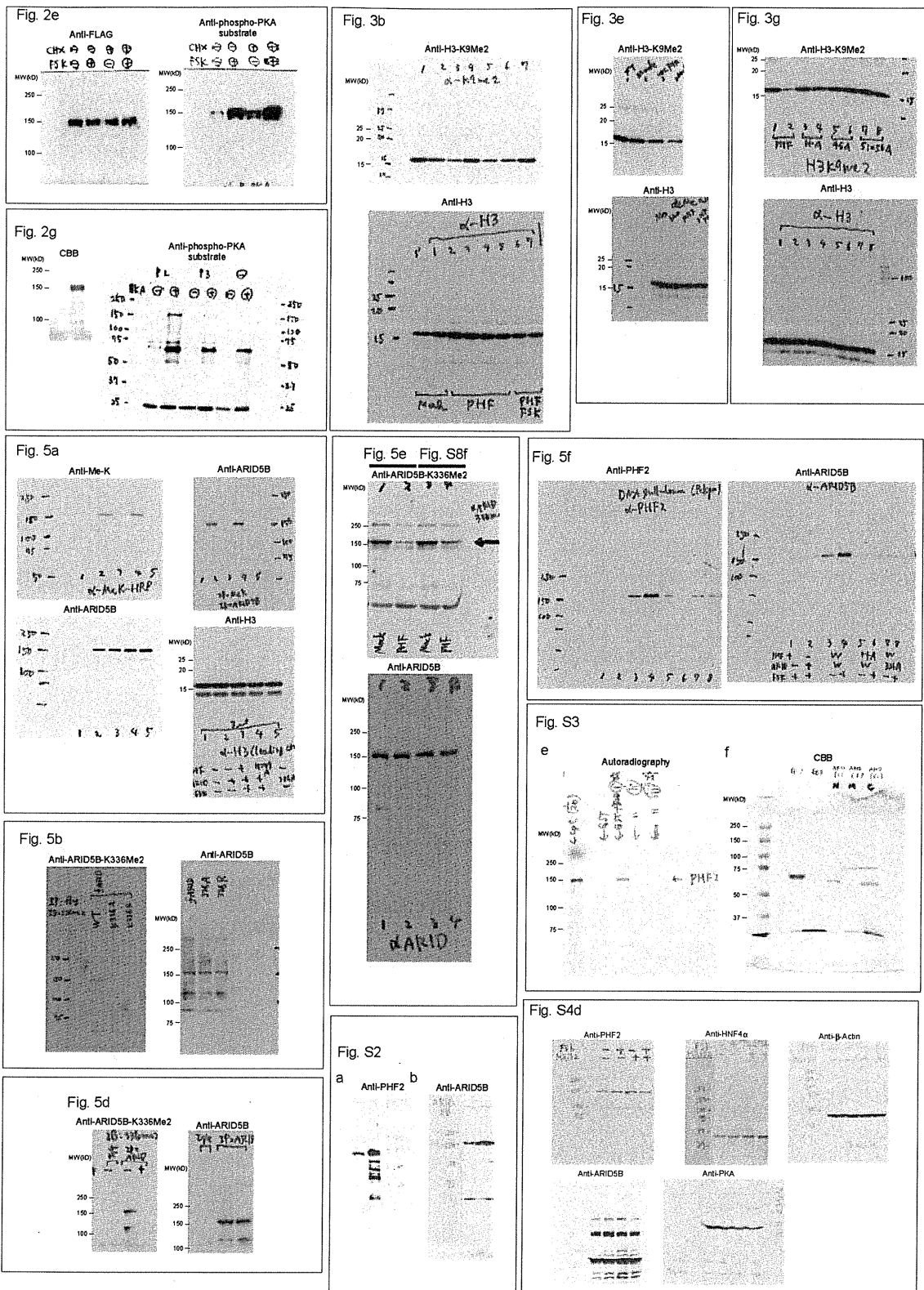


Figure S9 continued

Supplementary Table 1

Lists of antibodies, primers, and siRNA sequences used in this study.

Antibodies for immunoprecipitation

Antibody	Manufacture	Catalag No.	Lot No.
HNF4	Santa Cruz	H-171	K0204
FXR	Santa Cruz	H-130	K2805
FLAG M2	Sigma	F1804	088K6018
PHF2	Our laboratory		
ARID5B	Our laboratory		

Antibodies for Western blotting

Antibody	manufacture	Catalog No.	Lot No.	dilution
PHF2	Our laboratory			1/1000
ARID5B	Our laboratory			1/1000
FXR	Santa Cruz	sc1204	B052	1/500
RXR α	Santa Cruz	D-20	L210	1/1000
methyl-lysine	Abcam	ab23367	458685	1/300
FLAG	Sigma	F-7425	069K4767	1/1000
HA	Immunology Consultants Laboratory	RHGT-45A-4	22	1/1000

Antibodies for histone modification

Antibody	manufacture	Catalog No.	Lot No.	dilution
H3K9Me3	Abcam	ab6001	641998	1/1000
H3K9Me2	Abcam	1220	764743	1/1000
	Upstate	07-441	DAM1463717	1/1000
H3K9Me1	Upstate	07-450	DAM1394811	1/1000
H3K27Me3	Upstate	07-449	DAM1421462	1/1000
H3K27Me2	Upstate	07-452	24461	1/1000
H3K27Me1	Upstate	07-448	24439	1/1000
H3K4Me3	Upstate	07-473	131172	1/1000
H3K4Me2	Upstate	07-030,	DAM15170816	1/1000
H3K36Me3	Abcam	9050	826245	1/1000
H3K36Me2	Upstate	07-369	22475	1/1000
H3K79Me2	Abcam	ab3594	62690	1/1000
H4K20Me1	Upstate	07-748	30587	1/1000
H3	Abcam	ab1791	940500	1/2000

Primers for CHIP

mouse <i>Pepck</i> promoter	Fw	5'- TGTGCAGCCAGCAACATATGAA -3'
	Rv	5'- TGCAGGCTCTTGCCCTTAATTGTC -3'
mouse <i>G6Pase</i> promoter	Fw	5'- GTCAAGCAGTGTGCCCAAGTTAATA -3'
	Rv	5'- CCCAGCCCTGATCTTTGGAC -3'
mouse <i>Gapdh</i> promoter	Fw	5'- CCTGCTTATCCAGTCCTAGCTCA -3'
	Rv	5'- AAATGAGGCGGGTCCAAAG -3'

Primers for Realtime RT-qPCR

mouse <i>Pepck</i>	Fw	5'- GTGTTTGTAGGAGCAGCCATGAGA -3'
	Rv	5'- GCCAGGTATTTGCCGAAGTTGTAG-3'
mouse <i>G6Pase</i>	Fw	5'- GGATCCTGGGACAGACACACAA-3'
	Rv	5'- TGCAACACCTCTGGCCTCAC -3'
mouse <i>Hnf4a</i>	Fw	5'- CCGGGTGT CAGGAACAGTTG -3'
	Rv	5'- TGCAGGACAGTCTGAGCCATC -3'
mouse <i>Gapdh</i>	Fw	5'-AAATGGTGAAGGTCGGTGTG -3'
	Rv	5'-TGAAGGGGTCGTTGATGG -3'

Sequences of siRNA

mouse PHF2	# 1	5'-CAGCAAACCUGACUCGUUAAU -3'
	# 2	5'-GCAAAGGCUUGGAAAGAUCUU -3'
mouse ARID5B	# 1	5'-CCAAUCAUUUGACAUGUUCUU -3'
	# 2	5'-UCACAUGGGCGCAUUCUGAUU -3'
human PHF2	# 1	5'- GCAAGCGCCUGACGUCAAG -3'
	# 2	5'- AGGAGUUUGUGGACUAAUA -3'
human ARID5B	# 1	5'- UAACGGACCAGUUUGCAUU -3'
	# 2	5'- GCAGUCAACCCUAAACAGU -3'
mouse HNF4 α	# 1	5'- GAAGGAAGCUGUCCAAAAU -3'
	# 2	5'- AGAGGUCCAUGGUGUUUAA -3'

Endocrine disrupter bisphenol A increases *in situ* estrogen production in mouse urogenital sinus

BPA increases estrogen production

Shigeki Arase^{1,4}, Kenichiro Ishii^{1,4,5}, Katsuhide Igarashi², Kenichi Aisaki², Yuko Yoshio¹, Ayami Matsushima³, Yasuyuki Shimohigashi³, Kiminobu Arima¹, Jun Kanno², Yoshiki Sugimura^{1,*}

¹ Department of Nephro-Urologic Surgery and Andrology, Mie University Graduate School of Medicine, Mie, Japan

² Division of Cellular & Molecular Toxicology, National Institute of Health Sciences, Tokyo, Japan

³ Laboratory of Structure-Function Biochemistry, Department of Chemistry, Faculty of Sciences, Kyushu University, Fukuoka, Japan

* Correspondence to: Department of Nephro-Urologic Surgery and Andrology, Mie University Graduate School of Medicine, 2-174 Edobashi, Tsu, Mie 514-8507, Japan. Tel: +81-59-231-5026, Fax: +81-59-231-5203

E-mail: sugimura@clin.medic.mie-u.ac.jp

⁴ The first two authors contributed equally to this work.

⁵ Current address: Mie University Graduate School of Regional Innovation Studies, 1577 kurimamachiya-cho, Tsu, Mie 514-8507, JAPAN

Keywords: Bisphenol A; Urogenital sinus; *In situ* estrogen production; Aromatase; Steroidogenic enzyme

Abbreviations: EDC, endocrine-disrupting chemical; BPA, bisphenol A; DES, diethylstilbestrol; E₂, estradiol; UGS, urogenital sinus; UGE, urogenital sinus epithelium; UGM, urogenital sinus mesenchyme; Ad4BP/SF-1, adrenal-4 binding protein/steroidogenic factor-1; ERR γ , estrogen-related receptor γ .

Disclosure Summary: The authors have nothing to disclose.

Grant support: This study was supported by Grants-in Aid from the Ministry of Health, Labor and Welfare, Japan.

GEO accession number: GSE24928

ABSTRACT

The balance between androgens and estrogens is very important in the development of the prostate, and even small changes in estrogen levels, including those of estrogen-mimicking chemicals, can lead to serious changes. Bisphenol A (BPA), an endocrine-disrupting chemical (EDC), is a well-known, ubiquitous estrogenic chemical. To investigate the effects of fetal exposure to low-dose BPA on the development of the prostate, we examined the alterations of *in situ* sex steroid hormonal environment in the mouse urogenital sinus (UGS). In the BPA-treated UGS, E₂ levels and aromatase activity were significantly increased as compared with the untreated and DES-treated UGS. The mRNAs of steroidogenic enzymes, *Cyp19a1* and *Cyp11a1*, and sex-determining gene *Nr5a1* were up-regulated specifically in the BPA-treated group. The up-regulations of mRNAs were observed in the mesenchymal component of UGS (urogenital sinus mesenchyme; UGM), as well as in the cerebellum, heart, kidney, and ovary but not in the testis. The number of aromatase-expressing mesenchymal cells in the BPA-treated UGS was approximately twice compared to that in the untreated and DES-treated UGS. The up-regulation of *Esrrg* mRNA was observed in organs for which mRNAs of steroidogenic enzyme were also up-regulated. We demonstrated here that fetal exposure to low-dose BPA had the unique action which was the increases of *in situ* E₂ levels and CYP19A1 (aromatase) activity in the mouse UGS. Our data suggest that BPA might interact with *in situ* steroidogenesis by altering tissue components, such as the accumulation of aromatase-expressing mesenchymal cells, in particular organs.

INTRODUCTION

Endocrine-disrupting chemicals (EDCs) have been implicated to alter the fetal development of urogenital organs as well as the reproductive and endocrine systems in humans and other species [1]. The fetal development of urogenital organs is induced by endogenous hormonal messages that originate in fetal and maternal hormone systems. Fetal exposure to EDCs disrupts the interactions between endogenous hormones and their receptors, causing adverse effects later in life [2]. In the prostate, both androgens and estrogens play a significant role in development and differentiation as well as the maintenance of adult homeostasis [3]. Therefore, even small changes in estrogen levels, including estrogen-mimicking chemicals, can lead to changes in prostate development and differentiation.

Bisphenol A (BPA), one of the EDCs, is a well-known, ubiquitous estrogenic chemical used in the manufacture of polycarbonate plastics, as a lining in metal food and drink cans, and as dental sealants [4]. The concern with BPA originates from its detection in maternal and fetal plasma as well as the placenta [5] [6]. Thus, fetal exposure to BPA is implicated in fetal toxicity, as well as in subsequent growth of the infant. Histopathologically, fetal exposure to low-dose BPA (10 $\mu\text{g}/\text{kg}/\text{day}$) has been shown to increase cell proliferation of urogenital sinus epithelium (UGE) in the primary prostatic ducts of CD1 mice [7]. Recently, our group reported that fetal exposure to low-dose BPA (20 $\mu\text{g}/\text{kg}/\text{day}$) specifically increased the number of basal epithelial cells in the adult prostate of BALB/c mice, and also induced permanent cytokeratin 10 (KRT10) expression in such cells similar to the effects of synthetic estrogen diethylstilbestrol (DES, 0.2 $\mu\text{g}/\text{kg}/\text{day}$) [8]. Epigenetically, neonatal exposure of male rats to low-dose BPA (10 $\mu\text{g}/\text{kg}/\text{day}$) elicited critical molecular changes during prostate development and also increased prostatic gland susceptibility to precancerous neoplastic lesions and hormonal carcinogenesis [9]. Below 50 $\mu\text{g}/\text{kg}/\text{day}$, toxicological studies of BPA in rodent fetuses and offspring have demonstrated alterations of mammary gland development, open-field behavior, and reproductive functioning [10] [11] [12].

Some EDCs are reported to alter the *in situ* sex steroid hormonal environment in the reproductive system. The triazine herbicide atrazine binds directly to adrenal-4 binding protein/steroidogenic factor-1 (Ad4BP/SF-1, official symbol NR5A1) and increases CYP19A1 (aromatase) expression and ultimately estradiol (E_2) production in human genital cancer cell lines [13]. The aryl hydrocarbon (dioxin) also increases CYP19A1 (aromatase) expression mediated by its receptor in mouse ovaries [14]. In contrast, the phosphorothioate insecticide profenofos increases the expression of steroidogenic genes and testosterone (T) levels in rat testes [15]. Recently reported adverse effects of BPA on *in situ* steroidogenesis included increased T levels in mouse Leydig cells and decreased E_2 levels in porcine ovarian granulosa cells [16] [17]. Thus, BPA may have the potential to not only mimic estrogenic action but also alter *in situ* steroidogenesis in the prostate as well as other reproductive organs.

To investigate the effects of fetal exposure to low-dose BPA on *in situ* steroidogenesis in the developing prostate, we first measured sex steroid hormone levels and CYP19A1 (aromatase) activity in the BPA-treated mouse urogenital sinus (UGS), from which prostate develops embryologically. Subsequently, we examined the alterations of steroidogenic enzyme gene expression to confirm the alterations of the *in situ* sex steroid hormonal environment in the BPA-treated mouse UGS. Finally, we identified the BPA-specific biological effects for *in situ* steroidogenesis during fetal prostate development.

MATERIALS AND METHODS

Animals

Three female C57BL/6 mice (10 weeks of age) were mated with one male overnight, and then they were separated next morning (plug date denoted as day 0). In this study, 36 pregnant female C57BL/6 mice were purchased on the 12th day of gestation from Japan SLC (Shizuoka, Japan). All animals were housed individually in chip-bedded polyolefin cages in a room with controlled temperature ($23 \pm 1^\circ\text{C}$) and humidity ($45 \pm 65\%$) on a 12/12-h light/dark cycle. Mice were fed a phytoestrogen-low diet (NIH-07PLD; Oriental Yeast Co., Tokyo, Japan) and tap water *ad libitum*.

Chemicals

BPA and DES with a purity of $\geq 99\%$ were purchased from Nacalai Tesque (Kyoto, Japan) and Wako Pure Chemical Industries (Osaka, Japan), respectively.

Fetal exposure to chemicals

We randomly assigned 36 pregnant female C57BL/6 mice to three different treatment groups: i.e., BPA (20 $\mu\text{g}/\text{kg}/\text{day}$, $n = 12$) or DES (0.2 $\mu\text{g}/\text{kg}/\text{day}$, $n = 12$), which were dissolved in tocopherol-stripped corn oil (MP Biomedical Inc., Solon, OH, USA) by oral gavages, on embryonic day 13 (E13) to E16. For the control group, pregnant mice were fed tocopherol-stripped corn oil (2 ml/kg) ($n = 12$). Previously, our group reported that this protocol of fetal exposure to BPA and DES resulted in similar histopathological changes in adult prostate: i.e., increase of basal epithelial cell number and induction of cytokeratin 10 (KRT10), a classic marker associated with squamous differentiation, in such cells [8]. Our dose level of BPA was also based on reported results suggesting that BPA is < 100 -fold less potent than DES. The Mie University's Committee on Animal Investigation approved the experimental protocol.

Termination and UGS dissection

Between E17 and postnatal day 1 (P1), all animals were terminated by an overdose of isoflurane followed by cervical dislocation. For each group, $n = 15\sim 18$ fetuses (for both male and female) from 3 pregnant mice were collected at E17, E18, P0, and P1. The bladder and urethra were removed and dissected to isolate UGS, and then the 5~6 UGSs were pooled as 1 sample. Thus, the 15~18 UGSs were divided into 3 samples at each time point. The UGS, cerebellum, heart, kidney, testis, and ovary were collected in RNA *later* (Applied Biosystems, Foster City, CA, USA).

To isolate pure UGS, other tissues such as the bladder, urethra, Wolffian duct (WD), seminal vesicle (SV), and Mullerian duct (MD) were removed from both the male and female urogenital tracts. The histopathology of the mouse UGS was then examined by hematoxylin and eosin staining.

Measurements of in situ E_2 levels and CYP19A1 (aromatase) activity in UGS

E_2 levels and CYP19A1 (aromatase) activity in UGS were determined by liquid chromatography-tandem mass spectrometry (LC-MS/MS) [18] and a tritiated water release assay [19], respectively, which were made available by Aska Pharma Medical (Kanagawa, Japan). Briefly, the organs were homogenized, and the extracts were applied to a C18 Amprep solid-phase column (Amersham Biosciences, Arlington Heights, IL, USA) to remove contaminating fats. E_2 was then separated using a normal-phase high-performance liquid chromatography (HPLC) system (Jasco, Tokyo, Japan) with a silica gel column (Cosmosil 5SI; Nacalai Tesque, Kyoto, Japan), and 100 pg isotope-labeled [$^{13}\text{C}_4$]- E_2 was added to extracts. The evaporated extracts were reacted with 5% pentafluorobenzyl bromide/acetonitrile, under KOH/ethanol, for 1 h at 55°C. After evaporation, the products were reacted with 100 ml picolinoic acid solution (2% picolinoic acid, 2% 2-dimethylaminopyridine, and 1% 2-methyl-6-nitrobenzoic acid in tetrahydrofuran) and 20 ml triethylamine for 0.5 h at room temperature. The reaction products were dissolved in 1% acetic acid and were purified using a Bond Elute C18 column (Varian, Palo Alto, CA, USA). The products were measured with a reverse-phase LC (Agilent 1100, Agilent Technologies, Santa Clara, CA, USA) coupled with an API 5000 triple-stage quadrupole mass spectrometer (Applied Biosystems, Foster City, CA, USA) in the positive-ion mode. This device monitored the m/z 558 to m/z 339 (E_2) and m/z 562 to m/z 343 ([$^{13}\text{C}_4$]- E_2) transitions.

The tritiated water release assay was used for the measurement of CYP19A1 (aromatase) activity. This method measures the production of $^3\text{H}_2\text{O}$, which forms as a result of aromatization of the substrate [$1\text{b-}^3\text{H}$]-androst-4-ene-3,17-dione (New England Nuclear, Boston, MA, USA). Serum-free medium containing [$1\text{b-}^3\text{H}$]-androst-4-ene-3,17-dione solution (54 nM) was prepared, of which 0.5 ml was added to each sample. After incubation for 1 h, the samples were placed on ice and 200 μl of culture medium was

withdrawn. The medium was extracted with 500 μ l chloroform, vortexed, and then centrifuged for 1 min at 9000 \times g. A 100 μ l aliquot of the aqueous phase was mixed with 100 μ l of a 5% wt/vol charcoal 0.5% wt/vol dextran T-70 suspension, vortexed, and then incubated for 10 min. After centrifugation of the solution for 5 min at 9000 \times g, a 150 μ l aliquot was removed for measurement of radioactivity by liquid scintillation.

RNA extraction and cDNA preparation

Total RNA was extracted using the Qiagen mini RNA Easy kit in accordance with the manufacturer's instructions (Qiagen Inc., Valencia, CA, USA). The RNA concentration was then determined spectrophotometrically by multi-Detection Microplate Reader (Dainippon Sumitomo Pharma Co., Osaka, Japan). From 50 ng of total RNA, cDNA was reverse transcribed using oligo (dT) and Superscript II RNase H-reverse transcriptase (Invitrogen Co., Carlsbad, CA, USA) as previously described [8].

Analysis of gene expression profile

For determining gene expression profiles of the male UGS, GeneChip analysis with the Percellome method was performed [20]. Briefly, organs were prepared using RLT buffer (Qiagen Inc., Valencia, CA, USA). Total RNA was extracted using RNeasy Mini Kit (Qiagen Inc., Valencia, CA, USA). First-strand cDNA was synthesized by incubating 5 mg of total RNA with a T7 oligo (dT) primer (Invitrogen Co., Carlsbad, CA, USA) according to the manufacturer's protocol. The dsDNA was mixed with T7 RNA polymerase (Enzo Biochem., Farmingdale, NY, USA). During the *in vitro* transcription, generated cRNAs were labeled with biotin-16-UTP and biotin-11-CTP (Enzo Biochem., Farmingdale, NY, USA). The purified cRNA was fragmented at 300–500 bp into the target solution. Hybridization was performed with the GeneChip Mouse Genome 430 ver. 2.0 (Affymetrix Inc., Santa Clara, CA, USA) at 45°C for 18 h after staining with streptavidin-R-phycoerythrin conjugates (Molecular Probes, Invitrogen Co., Carlsbad, CA, USA). The reacted arrays were then scanned as digital image files, and the scanned data were analyzed with GeneChip Operating Software (Affymetrix Inc., Santa Clara, CA, USA). The expression data were converted to copy numbers of mRNA per cell by the Percellome method, quality controlled, and analyzed using Percellome software [20].

Real-time polymerase chain reaction (PCR) analysis

Real-time PCR was carried out in the iCycler iQ Detection System (Bio-Rad laboratories, Hercules, CA, USA) with iQ SYBR-Green Supermix reagents (Bio-Rad laboratories, Hercules, CA, USA) as previously described [8]. PCR amplification reaction was performed with specific primers as shown in Table 1. After PCR, melting curve analysis was performed to verify specificity and identity of the PCR products. All data were analyzed with the iCycler iQ Optical System Software Version 3.0A (Bio-Rad laboratories, Hercules, CA, USA). All the PCR data was normalized to *Gapdh* mRNA.

Preparation of primary cultured mesenchymal cells from UGS

UGS were dissected from the fetuses and separated into urogenital sinus epithelial (UGE) and urogenital sinus mesenchymal (UGM) components by tryptic digestion and mechanical separation as previously described [21]. UGM were cultured in RPMI-1640 with 5% FBS and plated out on 4-well glass slides (BD Falcon, Franklin Lakes, NJ USA). After several days, cells were fixed in methanol and processed for immunocytochemical analysis.

Immunocytochemical staining

The sections were first incubated for 15 min in 0.01 M PBS. After inhibition of endogenous peroxidases (10 min in 0.6% H₂O₂ diluted in 0.01 M PBS plus 0.2% Triton X-100, PBST), and saturation (2 h in a 5% normal goat serum solution), they were incubated overnight at 4°C in a polyclonal affinity-purified anti-aromatase antibody or ERR γ antibody raised in rabbit against quail recombinant aromatase or ESRRG diluted 1:500 in 0.01 M PBST. The next day the sections were immersed for 2 h at room temperature in a biotin-conjugated goat anti-rabbit IgG (DakoCytomation, Inc., Copenhagen, Denmark) diluted 1:400 in

PBST and subsequently for 2 h in a streptavidin-fluorescein complex (Rhodamine, DakoCytomation, Inc., Copenhagen, Denmark) diluted 1:50 in PBST. Between each step, sections were extensively rinsed in PBST. The sections were mounted onto microscope slides, coverslipped with a gelatin-based mounting medium, and stored in the dark at 4°C. For double-labeling immunofluorescence, Alexa Fluor 488-conjugated or 594-conjugated secondary antibodies were used. Rabbit polyclonal anti-aromatase antibody was kindly provided by Professor Nobuhiro Harada (Department of Biochemistry, Fujita Health University School of Medicine, Aichi, Japan) [22]. The rabbit polyclonal anti-ESRRG antibody used here was established and characterized as previously reported [23]. The mouse monoclonal anti-Ran antibody (Santa Cruz Biotechnology, Inc., Santa Cruz, CA, USA) was used to detect nucleus in cells. Ran, also called TC4, is the small RAS-related protein which is localized in nucleus.

Statistical analysis

The results were expressed as means \pm S.D. Differences among the three groups were determined using Student's *t*-test with Dunnett multiple comparison. $p < 0.05$ was considered statistically significant.

RESULTS

BPA-specific increases of E₂ levels and CYP19A1 (aromatase) activity in mouse UGS

The pregnant mice were exposed to low-dose BPA during the onset of prostatic budding (E13-E16), and UGS of fetuses was collected during bud elongation (E17-P1). In analyses of *in situ* sex steroid hormonal environment, E₂ levels and CYP19A1 (aromatase) activity were significantly increased only at P1 in BPA-treated UGS but not at P1 in the DES-treated UGS (Figure 1). At E17 and P1, both the E₂ levels and CYP19A1 (aromatase) activity in untreated male UGS were not significantly different compared with untreated female UGS.

BPA-specific up-regulations of steroidogenic enzyme and sex-determining gene mRNA in mouse UGS

To investigate the BPA-specific gene alterations related to increases of the E₂ levels and aromatase activity, we performed preliminarily GeneChip analysis with the Percellome method in the BPA-treated or DES-treated male UGS at E17 and P1. The results showed BPA-specific up-regulations of steroidogenic enzymes, such as *Cyp11a1*, *Cyp11b1*, and *Cyp17a1*, and sex-determining factors, such as *Nr5a1*, *Nr0b1*, *Gata4*, and *Amhr2* (data not shown). Furthermore, quantitative PCR analysis confirmed the mRNA up-regulations of *Cyp19a1*, *Cyp11a1*, and *Nr5a1* only in the BPA-treated neonatal (P0 and P1) UGS but not in the DES-treated neonatal UGS (Figure 2). There was no difference in mRNA expression levels between E17 and P1 when comparing the untreated male UGS to that of the female. In untreated male and female UGS, the mRNA of *Cyp19a1* was gradually increased between E17 and P1.

Restricted BPA-specific up-regulations of steroidogenic enzyme and sex-determining gene mRNA in mesenchymal component of UGS

In male fetuses at P1, it was not feasible to separate UGE and UGM components within the male UGS due to the formation of prostatic buds. In female at P1, the up-regulations of *Cyp19a1*, *Cyp11a1*, and *Nr5a1* mRNA were observed only in UGM but not in UGE of the BPA-treated group (Figure 3). In both the male and female UGE, expressions of such mRNAs were quite low and not up-regulated, even in the BPA-treated group. At E17, there was no difference in mRNA expression levels when comparing the untreated male UGM with that of the female.

BPA-specific increases of aromatase-expressing cells in primary cultured UGM

In both the male and female, P1 UGM was primary cultured *in vitro*. Representative pictures of aromatase-positive cells are shown in Figure 4A–4C. The aromatase-positive staining was observed in the cytoplasm of cultured UGM. The rate of positivity, i.e., percentage of cells that expressed CYP19A1 (aromatase) protein, was approximately 10% in the untreated and the DES-treated groups, whereas it was as high as approximately 30% in the BPA-treated group (Figure 4D). There was no difference in the rate of positivity of CYP19A1 (aromatase) when comparing the untreated male UGM to that of the female.